

1 **Swimming performance of *Bradyrhizobium diazoefficiens* is an**
2 **emergent property of its two flagellar systems**

3
4 **Supplementary Information**

5
6 J. Ignacio Quelas^a, M. Julia Althabegoiti^a, Celia Jimenez-Sanchez^{a,b}, Augusto A. Melgarejo^c,
7 Verónica I. Marconi^d, Elías J. Mongiardini^a, Sebastián A. Trejo^{e,f}, Florencia Mengucci^a,
8 José-Julio Ortega-Calvo^b, Aníbal R. Lodeiro^{a*}

9
10 ^aInstituto de Biotecnología y Biología Molecular (IBBM)-Facultad de Ciencias Exactas,
11 UNLP-CONICET (Argentina), ^bInstituto de Recursos Naturales y Agrobiología de Sevilla
12 (IRNAS)-CSIC (Spain), ^cDepartamento de Ciencias Básicas, Facultad de Ingeniería, UNLP
13 (Argentina), ^dFacultad de Matemáticas, Astronomía y Física (FAMAF)-UNC e IFEG-
14 CONICET (Argentina), ^eServei de Proteòmica i Biologia Estructural, Universitat Autònoma
15 de Barcelona, Bellaterra (Spain). ^fPresent address: Instituto Multidisciplinario de Biología
16 Celular (IMBICE), CONICET (Argentina).

17

18

19

20 **Matrix-assisted laser desorption ionization time-of-flight (MALDI-TOF) analysis of**
21 **subpolar and lateral flagellins.** Polypeptide samples were taken from single bands of
22 denaturing polyacrylamide gel (SDS-PAGE) separations of subpolar and lateral flagellin
23 subunits. These bands were trypsin-digested and analyzed essentially as described⁶⁰. For
24 MALDI-TOF target preparation, each sample was spotted onto a MALDI target plate (MTP)
25 384 GroundSteel plate (Bruker Daltonik, Bremen, Germany) using a standard dried droplet
26 method. Profile analyses were performed on an UltrafleXtreme MALDI TOF/TOF
27 spectrometer with FlexControl 3.4 (Bruker Daltonik, Bremen, Germany) data acquisition
28 software. Mass spectra were acquired in reflector mode geometry using the following
29 settings: 600-5000 Da mass range, positive mode, and ion suppression up to 800 m/z. Mass
30 calibration was performed using the Peptide Calibration Standard (Bruker Daltonik,
31 Bremen, Germany).

32 LafA1 and LafA2 (Bll6866 and Bll6865, respectively) were unambiguously
33 identified from the SDS-PAGE low-molecular-weight band by peptide mass fingerprint
34 MALDI TOF mass spectrometry (MS) using the MASCOT tools search. Similarly, only
35 some FliC proteins were identified from the SDS-PAGE high-molecular-weight band. A
36 further analysis that was carried out by sequencing MALDI TOF-TOF MS (Supplementary
37 Table S1) allowed a clear identification of specific tryptic peptides from each flagellin
38 (FliC1, FliC2, FliC3 and FliC4). The obtained chromatograms are shown in Supplementary
39 Fig. S1, and the specific peptides sequenced are resumed in Supplementary Table S2.
40 Therefore, all of the polypeptides that were encoded in bll6865-bll6866 and bll5843-bll5846
41 were identified in our *B. diazoefficiens* flagellin samples.

42

43 Table S1. Peptides identified in theoretical tryptic digestion of flagellins*.

	Meas M/z	Calc MH+	Dev.(Da)	Range	Sequence
637373431 NP_772483 [B. japonicum USDA 110: NC_004463]					
peak 40	2454,40	2454,37	0.034	741 - 763	QSIAVSALSANQSQSVLQLLR
peak 17	1681,95	1681,88	0.070	93 - 108	SIANQALQTTVGYSTK
peak 38	2336,20	2336,16	0.041	36 - 56	KVNTALDNPTNFFTAQGLDNR
peak 29	2208,10	2208,07	0.035	37 - 56	VNTALDNPTNFFTAQGLDNR
peak 11	1616,92	1616,86	0.061	689 - 704	SEGSALGSNLSIVQVR
peak 28	2102,15	2102,11	0.038	12 - 30	QNLLSLQSTADLLATTQER
peak 46	2632,30	2632,29	0.008	501 - 526	TLTFTSFNGGTPVNVTFDGDGTNGTVK
peak 49	2734,43	2734,39	0.035	347 - 373	STTAGSLGTLVQDGSSTLNIDGHTITFK
peak 63	3746,28	3746,01	0.271	1 - 35	MSNIVLSASVRQNLLSLQSTADLLATTQERLSTGK
637373432 NP_772484 [B. japonicum USDA 110: NC_004463]					
peak 35	2311,14	2311,10	0.041	36 - 56	SVNSALDNPTNFFTAQSLDNR
peak 27	2087,15	2087,11	0.045	12 - 30	QNLLSLQSTADLLATTQNR
peak 40	2454,40	2454,37	0.034	735 - 757	QSIAVSALSANQSQSVLQLLR
peak 47	2647,39	2647,36	0.029	337 - 363	TTSAASLGATIADGSTLNVDGHHVITFK
peak 32	2273,20	2273,17	0.038	628 - 648	LVFDETGKSSLNITGVTYNSK
peak 17	1681,95	1681,88	0.070	93 - 108	SIANQALQTTVGYSTK
peak 14	1646,95	1646,87	0.078	683 - 698	SEASSLGSNLSVVQIR
peak 5	1359,81	1359,76	0.046	670 - 682	VLTNLNAASSTLR
peak 22	1817,05	1816,95	0.103	318 - 336	ALGLTTSTGAGNATVNVNR
peak 50	2915,61	2915,57	0.046	268 - 300	TVSISGAATIIVSASQPGAIVSTAAAGAVTLK
peak 42	2573,40	2573,39	0.007	12 - 35	QNLLSLQSTADLLATTQNRSLSTGK
peak 1	932,56	932,51	0.056	521 - 528	TLDQLNTK
peak 7	1383,73	1383,71	0.015	636 - 648	SSLNITGVTYNSK
637373433 NP_772485 [B. japonicum USDA 110: NC_004463]					
peak 35	2311,14	2311,10	0.041	36 - 56	SVNSALDNPTNFFTAQSLDNR
peak 21	1785,04	1784,96	0.077	318 - 336	ALGLTTAVGGGNATVNVNR
peak 40	2454,40	2454,37	0.034	735 - 757	QSIAVSALSANQSQSVLQLLR
peak 47	2647,39	2647,36	0.029	337 - 363	TTSAASLGATIADGSTLNVDGHHVITFK
peak 32	2273,20	2273,17	0.038	628 - 648	LVFDETGKSNLSITGVTYNSK
peak 17	1681,95	1681,88	0.070	93 - 108	SIANQALQTTVGYSTK
peak 25	2060,14	2060,10	0.042	12 - 30	QNLLSLQSTADLLATTQSR
peak 15	1660,97	1660,89	0.082	683 - 698	SEASSLGSNLTIVQVR
peak 43	2576,29	2576,26	0.025	495 - 520	TLTFASFNGGTAIVNVTFDGDGTNGTVK
peak 34	2293,16	2293,18	-0.022	683 - 703	SEASSLGSNLTIVQVRQDFNK
peak 6	1375,80	1375,75	0.050	670 - 682	VLTNLNSASSTLR
peak 57	3374,92	3374,79	0.128	649 - 682	GLGLAALTGGVDFIDNAATNKVLTNLNSASSTLR
peak 62	3492,98	3492,79	0.185	448 - 484	LSTGVNADLSVTGTGNALNVLGLAGNTGTSTAFTAAR
peak 23	2018,11	2018,06	0.052	649 - 669	GLGLAALTGGVDFIDNAATNK
peak 52	3038,66	3038,61	0.050	57 - 86	ASDINNLLDGIANGVQVLQAANTGITSLQK
peak 36	2325,34	2325,29	0.050	313 - 336	ADLLKALGLTTAVGGGNATVNVNR
peak 60	3428,99	3428,83	0.153	301 - 336	SSTGADLSVTGKADLLKALGLTTAVGGGNATVNVNR
peak 9	1563,89	1563,80	0.088	109 - 124	SNVSTTISGATAADLR
peak 50	2915,61	2915,57	0.046	268 - 300	TVSISGAATIIVSASQPGAIVSTAAAGAVTLK
peak 61	3433,88	3433,72	0.153	485 - 520	TSGVGGITGKTLTFASFNGGTAIVNVTFDGDGTNGTVK
peak 41	2546,25	2546,38	0.127	12 - 35	QNLLSLQSTADLLATTQSRSLSTGK
peak 1	932,56	932,51	0.056	521 - 528	TLDQLNTK
peak 7	1383,73	1383,71	0.015	636 - 648	SNLSITGVTYNSK
peak 63	3746,28	3745,92	0.362	409 - 447	AIDLATGVQATINANGTATLATATGQTNSINASGQLK

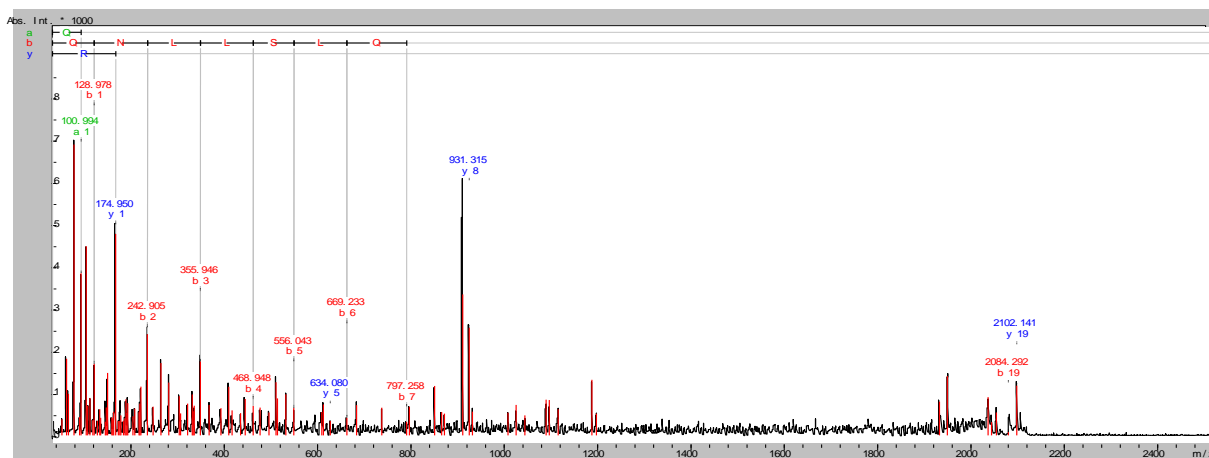
637373434 NP_772486 [B. japonicum USDA 110: NC_004463]					
peak 35	2311,14	2311,10	0.041	36 - 56	SVNSALDNPTNFFTAQSLDNR
peak 21	1785,04	1784,96	0.077	318 - 336	ALGLTTAVGGGNATVNVNR
peak 31	2265,18	2265,15	0.034	683 - 703	SEASSLGSNLSVVQVRQDFNK
peak 27	2087,15	2087,11	0.045	12 - 30	QNLLSLQSTADLLATTQNR
peak 40	2454,40	2454,37	0.034	735 - 757	QSIAVSALSANQSQSVLQLLR
peak 47	2647,39	2647,36	0.029	337 - 363	TTSAASLGATIADGSTLNVDGHVITFK
peak 13	1632,94	1632,86	0.081	683 - 698	SEASSLGSNLSVVQVR
peak 4	1345,79	1345,74	0.049	670 - 682	VLSNLNAASSTLR
peak 32	2273,20	2273,17	0.038	628 - 648	LVFDETGKSNLSITGVTYNSK
peak 17	1681,95	1681,88	0.070	93 - 108	SIANQALQTTVGYSTK
peak 43	2576,29	2576,26	0.025	495 - 520	TLTFASFNGGTAVNVTFDGDGTNGTVK
peak 24	2048,12	2048,07	0.054	649 - 669	GLGLAALTSGVDFIDNAATNK
peak 57	3374,92	3374,79	0.128	649 - 682	GLGLAALTSGVDFIDNAATNKVLSNLNAASSTLR
peak 62	3492,98	3492,79	0.185	448 - 484	LSTGVNADLSVTGTGNALNVLGLAGNTGTSTAFTAAR
peak 52	3038,66	3038,61	0.050	57 - 86	ASDINNLLDGIANGVQVLQAANTGITSLQK
peak 36	2325,34	2325,29	0.050	313 - 336	ADLLKALGLTTAVGGGNATVNVNR
peak 8	1533,86	1533,79	0.076	109 - 124	SNVSATISGATAADLR
peak 60	3428,99	3428,83	0.153	301 - 336	SSTGADLSVTGKADLLKALGLTTAVGGGNATVNVNR
peak 51	2959,61	2959,58	0.028	670 - 698	VLSNLNAASSTLRSEASSLGSNLSVVQVR
peak 50	2915,61	2915,57	0.046	268 - 300	TVSISGAATIIVSASQPGAASVSTAAAGAVTLK
peak 61	3433,88	3433,72	0.153	485 - 520	TSGVGGITGKTLTFASFNGGTAVNVTFDGDGTNGTVK
peak 42	2573,40	2573,39	0.007	12 - 35	QNLLSLQSTADLLATTQNRSLTGK
peak 55	3190,69	3190,62	0.072	704 - 734	SLINVLTGTGSSNLTADTNTTEAANSQALSTR
peak 1	932,56	932,51	0.056	521 - 528	TLDQLNTK
peak 7	1383,73	1383,71	0.015	636 - 648	SNLSITGVTYNSK
peak 64	3746,28	3745,92	0.362	409 - 447	AIDLATGVQTATINANGTATLATATGQTNSSINASGQLK
peak 66	3824,33	3824,00	0.328	87 - 124	LIDSAKSIANQALQTTVGYSTKSNVSATISGATAADLR
peak 65	3823,25	3822,91	0.343	699 - 734	QDFNKSLINVLTGTGSSNLTADTNTTEAANSQALSTR
peak 63	3592,05	3591,87	0.179	670 - 703	VLSNLNAASSTLRSEASSLGSNLSVVQVRQDFNK

44

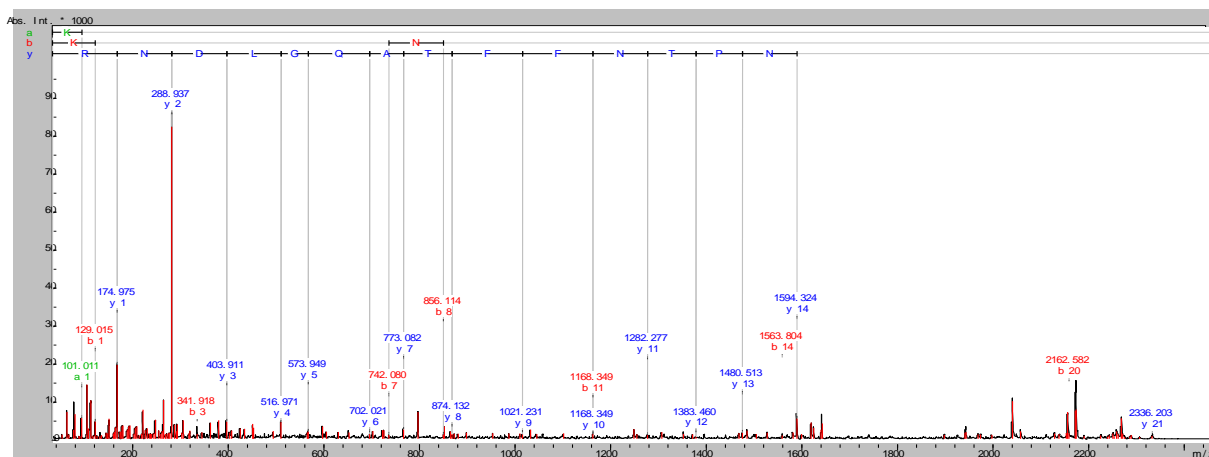
45 *All matches between spectrum mass peak and theoretical tryptic digest peptides of each
46 flagellin are shown. Grey rows: specific peptides from each flagellin. Specific peptide
47 corresponds to sequences present only in one flagellin but not in the others.

48

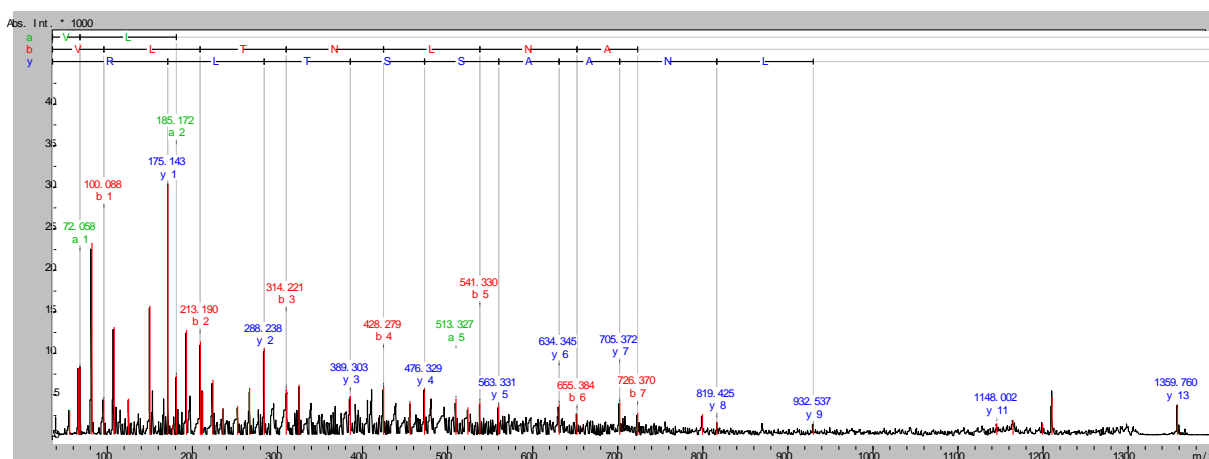
49

50 **637373431 NP_772483:**51 **Peak 28**

52

53 **Peak 38**

54

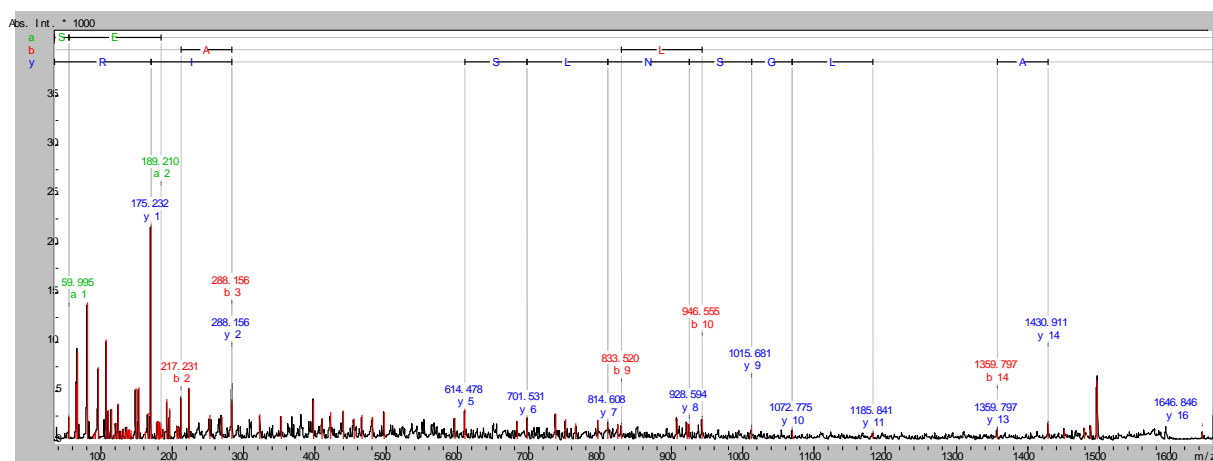
55 **637373432 NP_772484:**56 **Peak 5**

57

58

Figure S1

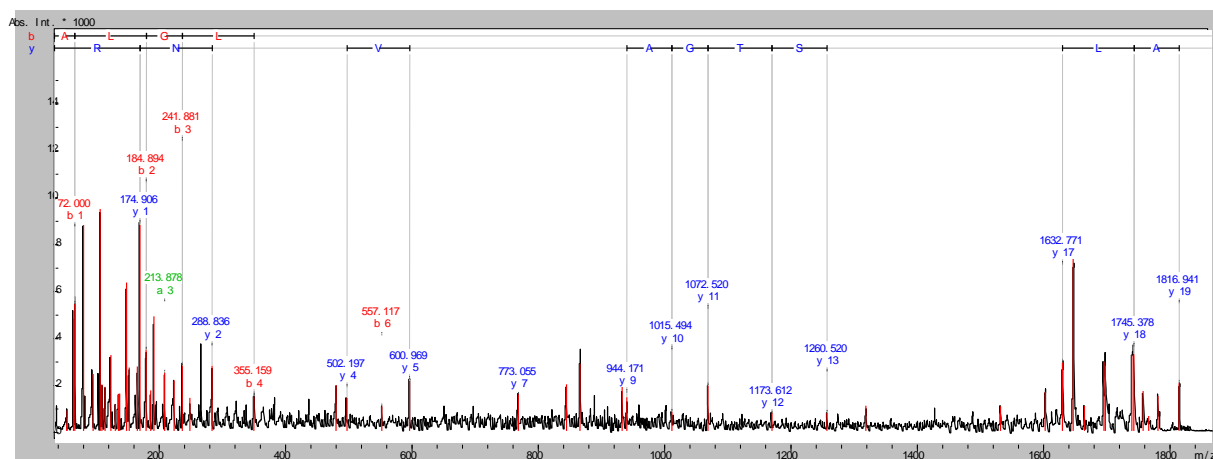
59 Peak 14



60

61

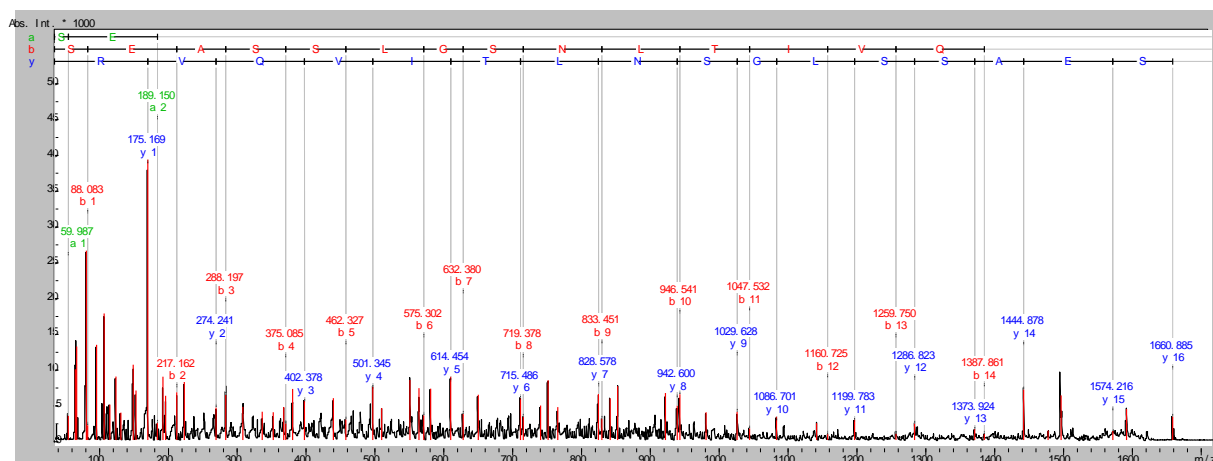
62 Peak 22



63

64 **637373433 NP_772485:**

65 Peak 15

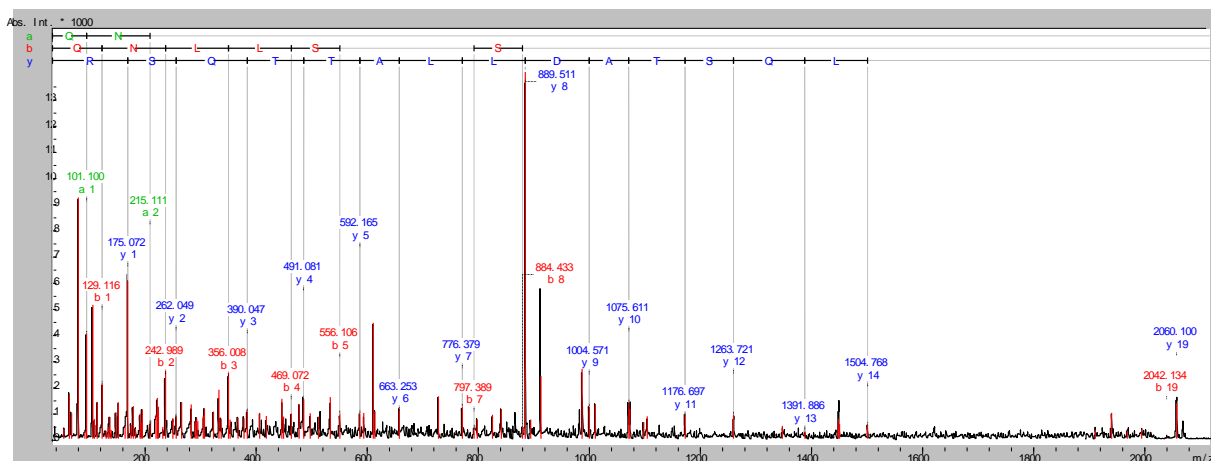


66

67

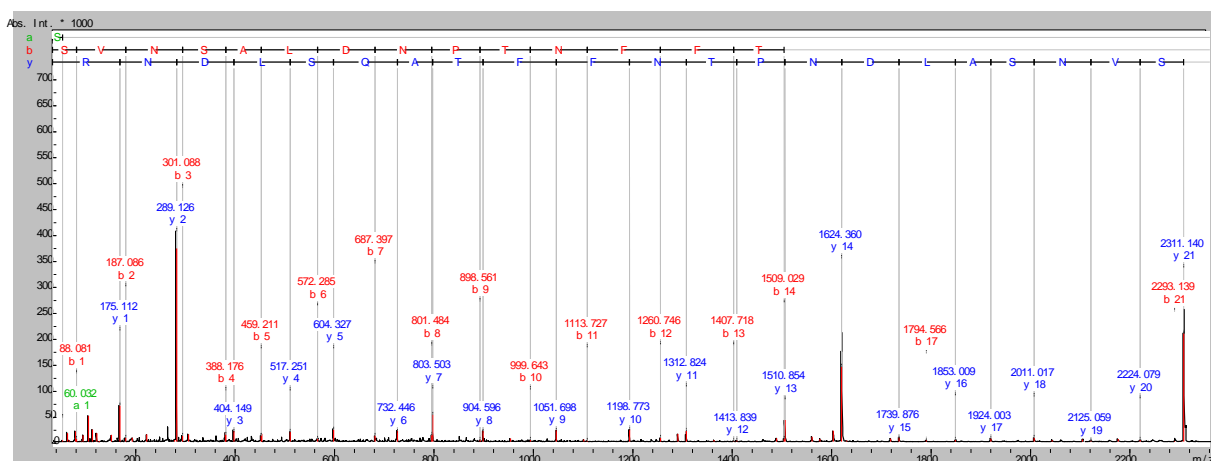
Figure S1 (cont.)

68 Peak 25



69

70 Peak 35

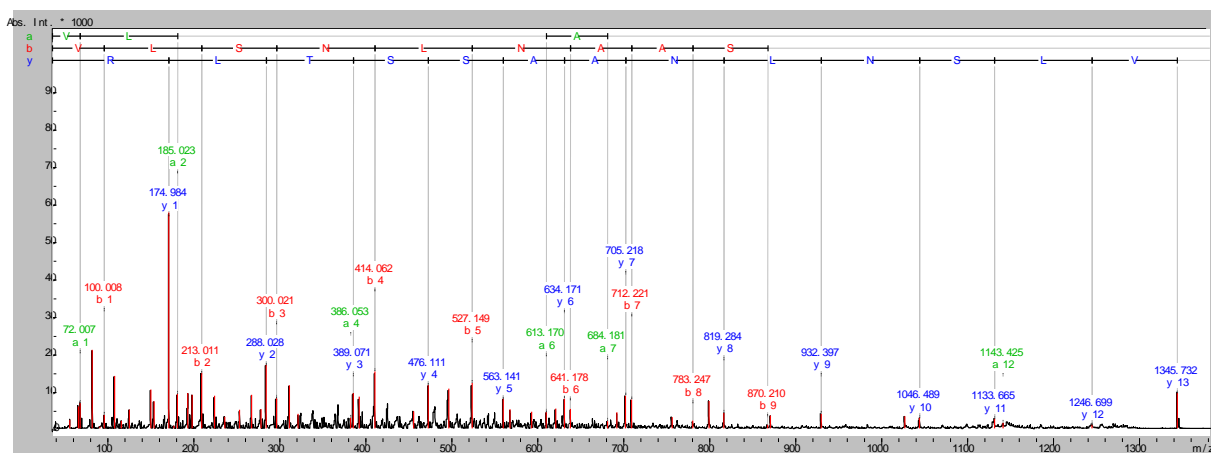


71

72

73 637373434 NP_772486:

74 Peak 4

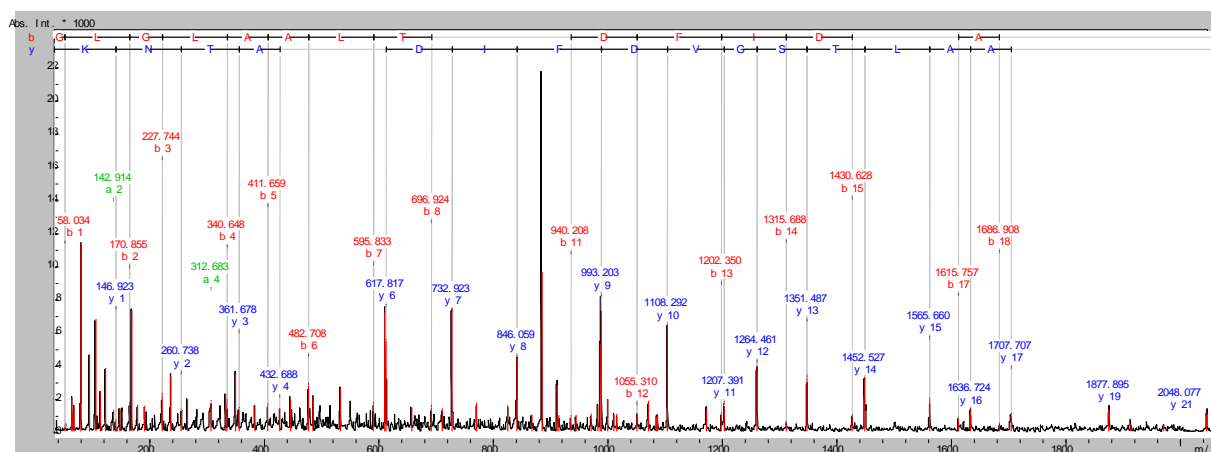


75

76

Figure S1 (cont.)

77 Peak 24



78

79 **Fig. S1.** Sequencing of the specific peptides of each flagellin by MALDI TOF-TOF MS². Sequence assignment was performed
 80 using Biotoools 3.2 SR4 software with a tolerance of 0.6 Da for internal fragment assignments and 0.15 Da for parental peak.
 81 Specific peptide sequencing was used to identify each flagellin with a high confidence degree.

82

83

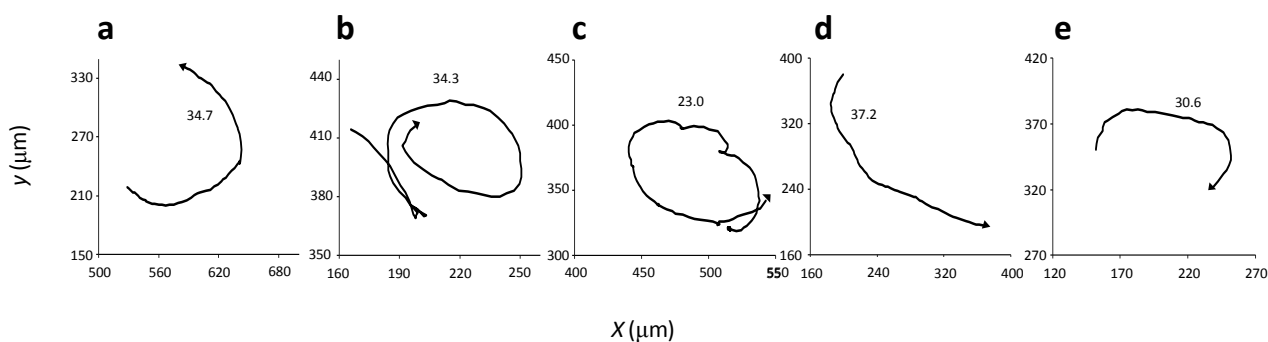
84 **Table S2.** Specific unique peptides from *FliC1*, *FliC2*, *FliC3* and *FliC4* sequenced by MALDI
 85 TOF-TOF.

Flagellins	Meas M/z	Calc MH+	Dev.(Da)	Range	Sequence
FliC1 637373431 NP_772483 [B. japonicum USDA 110: NC_004463]					
peak 28	2102,15	2102,11	0.038	12 - 30	QNLLSLQSTADLLATTQER
peak 38	2336,20	2336,16	0.041	36 - 56	KVNTALDNPTNFFTAQGLDNR
FliC2 637373432 NP_772484 [B. japonicum USDA 110: NC_004463]					
peak 5	1359,81	1359,76	0.046	670 - 682	VLTNLNAASSTLR
peak 14	1646,95	1646,87	0.078	683 - 698	SEASSLGSNLSVVQIR
peak 22	1817,05	1816,95	0.103	318 - 336	ALGLTTSTGAGNATVNVNR
FliC3 637373433 NP_772485 [B. japonicum USDA 110: NC_004463]					
peak 15	1660,97	1660,89	0.082	683 - 698	SEASSLGSNLTIVQVR
peak 25	2060,14	2060,10	0.042	12 - 30	QNLLSLQSTADLLATTQSR
peak 35	2311,14	2311,10	0.041	36 - 56	SVNSALDNPTNFFTAQSLDNR
FliC4 637373434 NP_772486 [B. japonicum USDA 110: NC_004463]					
peak 4	1345,79	1345,74	0.049	670 - 682	VLSNLNAASSTLR
peak 24	2048,12	2048,07	0.054	649 - 669	GLGLAALTSGVDFIDNAATNK

86

87

88 **Some trajectories are difficult to classify.** The complexity of the trajectories observed in
 89 this work prevented us to classify them without a quantitative criterion. Examples of
 90 trajectories that contained different features and could not be unambiguously classified are
 91 presented in Supplementary Fig. S2.



92

93 **Fig. S2.** Examples of trajectories difficult to classify in the classes defined in the main article: curved (a), linear with RR
 94 changes in direction and then circular (b); circular with an RRF change in direction (c); wide open curve (d); curved with a
 95 linear stretch in the middle (e). Coordinate axis values correspond to those of Fig. 2a-d in the main text. The numbers next
 96 to the trajectories indicate the mean speeds in micrometers per second ($\mu\text{m}\cdot\text{s}^{-1}$).

97

98 **Values of Trajectory Index (*TRAIN*) for the trajectories shown in the main article.** To
 99 better illustrate how *TRAIN* was calculated, we present in Supplementary Table S3 the
 100 values of all the variables that gave rise to *TRAIN* in the trajectories shown in Figs. 2, 4 and
 101 S2. In this way, the reader may contrast the numerical values of *NGDR*, *s*, $\langle \cos\alpha \rangle$ and *c*
 102 against the trajectories to appreciate the extent to which *TRAIN* represents their shapes.

103

104

Table S3. TRAIN calculation of the trajectories exemplified in this work*

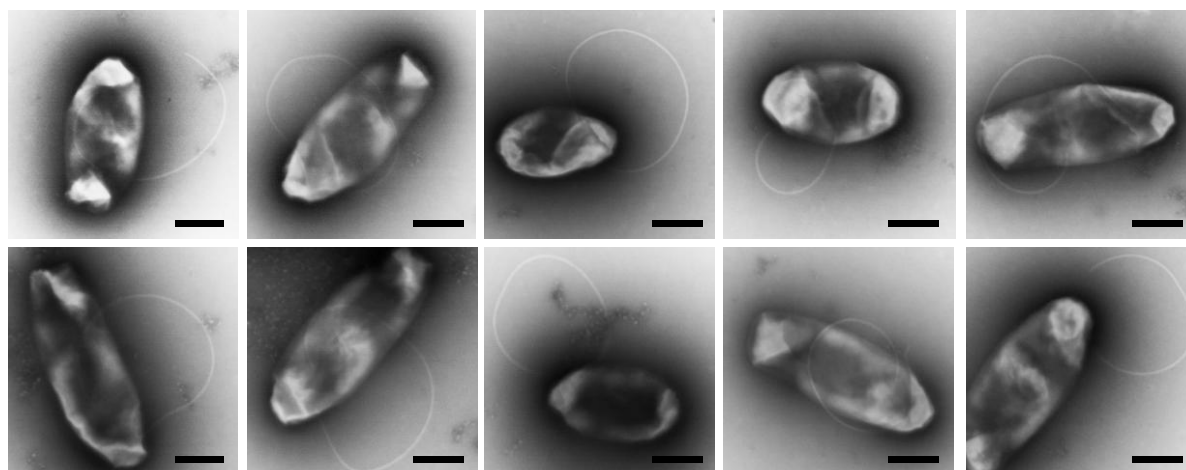
Trajectory	TRAIN variables				TRAIN
	NGDR	<i>s</i>	$\langle \cos\alpha \rangle$	<i>c</i>	
Circular (2e)	0.13	1.18	0.95	0	1.09
Circular (4a)	0.12	0.77	0.98	0	1.19
Linear (2f)	0.97	0.34	0.95	0	1.99
RRF (2h)	0.20	1.91	0.89	5	0.60
RRF (4d)	0.13	4.56	0.80	7	0.21
RRF (4g)	0.60	2.78	0.90	2	1.06
RR (2g)	0.55	6.17	0.86	7	0.36
Rough (2i)	0.54	1.25	0.23	29	0.46
Diffusive (2j)	0.12	6.14	0.32	49	$2 \cdot 10^{-6}$
Curved (S2a)	0.51	0.72	0.98	0	1.62
Circular/RR (S2b)	0.10	3.80	0.92	3	0.78
Circular/RRF (S2c)	0.11	4.17	0.91	3	0.76
Wide open curve (S2d)	0.85	0.34	0.98	0	1.94
Curved/linear (S2e)	0.56	0.91	0.97	0	1.59

105

$$*TRAIN = NGDR^s + \langle \cos\alpha \rangle^c$$

106

107 **More images of Δ lafA cells from soft agar plates with viscosity at 80 mPa s.** These
 108 transmission electron micrographs show the reproducibility of the flagellar sizes and
 109 disposition with respect to the cell body.



110

111 **Fig. S3.** Ten Δ lafA cells with short and curved subpolar flagella, often surrounding the cell body (scale bar: 0.5 μ m).

112 **References**

- 113 60. Watt, S. A., Patschkowski, T., Kalinowski, J. & Niehaus, K. Qualitative and quantitative
114 proteomics by two-dimensional gel electrophoresis, peptide mass fingerprint and a
115 chemically-coded affinity tag (CCAT). *J. Biotechnol.* **106**, 287-300;
116 DOI:10.1016/j.jbiotec.2003.07.014 (2003)

117